

New Technique for Vibration Damping of Cantilevered Plate

Eng. anwar M. anwar¹
Dep. of Mech Engineering
Military Tech. College
Cairo, Egypt

Prof.Dr. adel omar abdelrazek²
Dep. of mech Engineering
Military Tech. College
Cairo, Egypt

Dr. Ahmed.hassan³
Dep. of Mech Engineering
Military Tech. College
Cairo, Egypt

Prof.Dr. mostafa adnan⁴
Dep. of A/C. Engineering
Military Tech. College
Cairo, Egypt

Abstract— A new technique of structural damping treatments is introduced. This technique is the pretension layer damping (PTLD), which consists of two elastic damping material, pretension and perfectly bonded to both sides of the base structure. The pretension layer generates an axial uniformly distributed superficial damping force. The percentage of pretension is increased and the performance characteristic is monitored for cantilever plate treated by PLTD. The obtained results indicate that there is good attenuation percentage between untreated and treated plate. It is also noted that the higher the superficial force value, the higher the attenuation percentage. The used technique is a passive technique, which means that it is simple, reliable, and need no complex circuits compared with other active approaches

Keywords—vibration; structure; sandwich; honeycomb; static; modal.

I. INTRODUCTION

Vibration and vibration control of structures are among the major research subjects in mechanical engineering, aerospace engineering, civil engineering, engineering mechanics and related technical disciplines, and are vital to many industrial and defense-related applications[1]. Passive constrained layer damping (PCLD) treatments have been utilized as a simple, reliable and low cost means for damping out the vibration of many flexible structure[2, 3]. However, for effective performance over a broad range of temperature and frequencies, the weight of PCLD treatments can lead to serious limitation in use with application where weight is critical[4]. Conventional structural designs are often unacceptable in coping with modern problems of structural resonance caused by the complex nature of the dynamic environments and the requirements of design objectives, including low noise, light weight, long life and increased reliability[5]. These requirements have motivated a new approach to structural design where feedback control principles and advances in sensors and actuators are applied to the design of high performance structural systems. The controlled structure may be composed of a conventional structure and a separate and distinct control system; or it may be an active structure[6]. The active structure is a controlled structure that contains sensors and/ or actuators that are highly integrated into the structure and have structural functionality in addition to control functionality[7-10]. In the present paper, a new technique of structural damping treatments is introduced. This technique is the pretension layer damping (PTLD), which consists of two elastic damping material, pretension and perfectly bonded to both sides of the base structure. The pretension layer generates an axial uniformly

distributed superficial damping force. These forces have a complex form by virtue of its complex Young's modulus. The vertical components of the real part of these complex forces always tend to straighten the elastic line of the vibrating plate, while the imaginary parts have a damping nature depending on the initial strain value as well as the damping loss factor of the damping material. These two parts of the induced superficial forces play an important role in the reduction of the plate vibration amplitudes.

The theoretical response of the (PTLD) model, is compared with the experimental response of a base excited cantilevered plate fully treated with (PTLD) technique, using two layers of elastic damping material that are pre-tensioned within their elastic range[11]. The two pre-tensioned damping layers are perfectly bonded to both sides of the cantilevered plate, to generate an axial uniformly distributed superficial damping force. It will be shown that with such passive control capabilities, the damping characteristics of the plate vibration are improved. The Plate/PTLD system is tested at different pre-strain levels, (i.e., at different superficial forces). Thus, the effect of the (PTLD) treatment on the system response is presented at different control forces. The experimental setup is described in details. The natural frequencies of a plain plate and the Plate/PTLD system are obtained experimentally, showing that there is almost no change in the natural frequency of the structure due to this treatment. This indicates that the (PTLD) treatment does not change the system mechanical properties. Moreover the loss factor and Young's modulus of the plain Plate and the Plate/PTLD system are determined experimentally, since their values are necessary for the theoretical analysis.

2. Mechanical Properties of the Tested Structure

The proposed Plate/PTLD system consists of a plate, which is treated by two layers of elastic rubber material. The two rubber layers are stretched identically within their elastic range, then they are perfectly bonded to both sides of the vibrating plate, with high accuracy to the symmetry of bonding, to generate equally distributed constant forces on the superficial fibers of the two opposing faces of the vibrating plate. The plain plate and the layers of the elastic damping materials, used in this technique, are not standard materials. Accordingly it is necessary to determine their mechanical properties experimentally.

3. Mechanical Properties of the Cantilevered Plain Plate

It is important to determine the mechanical properties of the plain plate (density, Young's modulus and loss factor) including natural frequencies, which will facilitate the assessment of the performance of the (PTLD) treatment and its effect on the frequency response.

3.1. Determination of the natural frequencies of the plain plate

The plain plate is cut from a sheet of metal alloy of thickness 1.2 mm, with the dimensions shown in Figure (1).

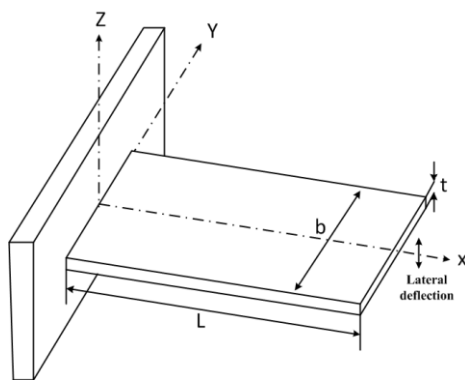


Fig. (1) Dimensions of the plain plate used in the experiments

The proposed sample plain plate is fixed into a steel base using four screws, and the base is mounted on the push rod of electromagnetic shaker (type 4808 B&K), as shown in Figure (2).

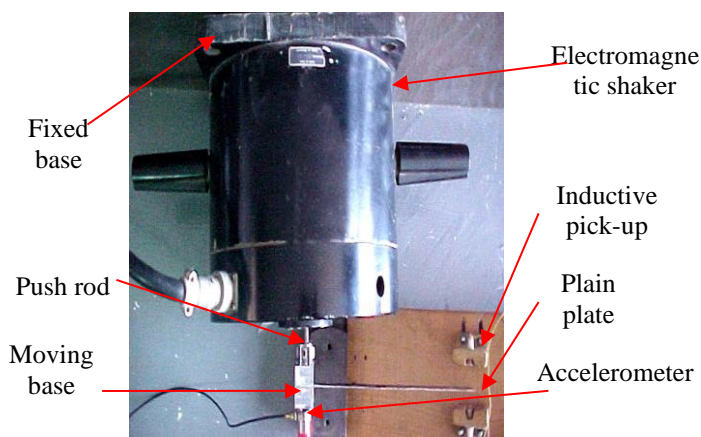


Fig. (2) Sample plain plate fixed into the push rod of the shaker via a metallic base

3.1.1. Sine Sweep of Structure

As shown in Figure (3), NI system with lab view program is fed to the shaker via a power amplifier (Type 2712 B&K).

The shaker excites the base of the sample plain plate through the push rod, where an accelerometer (Type 4367 B&K) is mounted on the moving base. A signal, proportional to the acceleration of the base is fed to a charge amplifier (Type 2635 B&K), where the signal is integrated twice to give the displacement of the base. The signal representing the base displacement is passed lab view program. The tip displacement of the plain plate is measured by two accelerometers, which produces a signal proportional to the tip displacement of the plain plate. The frequency is swept automatically over a frequency range from 1Hz up to 100 Hz. Since the base and the tip displacements of the cantilevered plain plate are synchronized, the transfer function representing the absolute tip displacement of the plain plate to its base displacement can be plotted in lab view. Figure (4) represents the measured transfer function and the corresponding phase angle of the cantilevered sample plain plate. It is shown from the graph of the transfer function that the first natural frequency of the plain plate is (10.82 Hz).

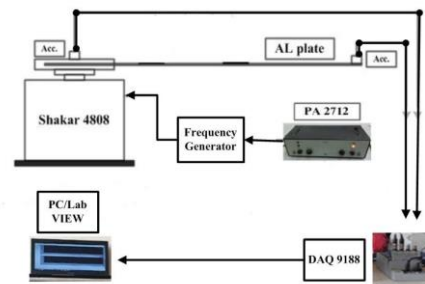


Fig. (3) Schematic drawing of test set-up and instrumentation

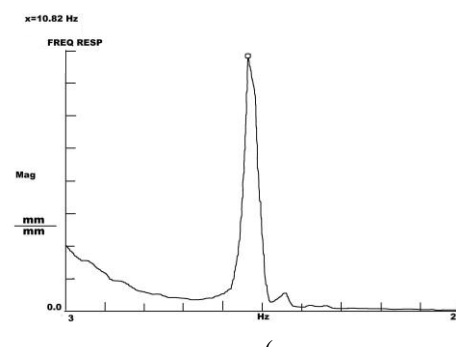


Fig. (4) The transfer function of the sample cantilevered plain plate

3.2. Determination of Young's modulus of the plain plate

One of the significant mechanical properties of the materials is the Young's modulus or the modulus of elasticity. Several investigators have used various

methods for the determination of this dynamic property either by using tension-compression machines or by exciting the specimens in bending.

Using the equation representing the cantilevered plain plate eigen values

$$E_3' = (2\pi\omega_n)^2 \frac{\rho_3 A_3}{I_3 \beta_n^4} \quad (1)$$

Where " ω_n " is the n^{th} natural frequency of the plate, " ρ_3 " is the specific mass of the plate material (density), " A_3 " is the plate cross section area, " I_3 " is the second moment of inertia of the plate cross-section area about the "z-axis" and " β_n " is determined from the roots of the transcendental equation of a cantilevered plain plate, which are obtained from reference tables based on the boundary conditions of the structural element and the vibrating mode. From equation (1), it is clear that the determination of Young's modulus of the plain plate material requires the determination of the plain plate natural frequencies. The first natural frequency of the cantilevered sample plain plate was found to be 10.82 Hz as shown in Figure (4). From reference tables, the first root of the transcendental equation of the cantilevered plain plate is " $\beta_1 L = 1.875$ ". Substitution in equation (1), it gives $E_3' = 68.2 GPa$

4.3. Measurement of the Damping Loss Factor of the Plain Plate

There exist a number of modal analysis methods, which, although their difference in details, share the same basic assumption, namely, that in the vicinity of a resonance, the total response is dominated by the contribution of the mode whose natural frequency is closest. The methods vary as to whether they assume that all the response is attributed to that single mode or whether the other modes contributions are represented by a simple approximation.

Perhaps the simplest of this methods is one which has been used for a long time and which is sometimes referred to as "the peak amplitude" or "the half power" method. This is a method, which works adequately for structures whose FRF exhibit well separated modes, [15]. Figure (5) shows the well separation between the first two modes of the proposed plain plate. The "Half Power Method" is applied and the damping loss factor of the mode in question can now be estimated as

$$\eta_n = \frac{\omega_a^2 - \omega_b^2}{\omega_n^2} \quad (2)$$

For the proposed cantilevered plain plate, its loss factor can be calculated using equation (2), where the half power method is applied to the graph shown in Figure (4), or it can be calculated automatically using lab view ,

where the damping loss factor of the plain plate at the first resonance was " $\eta_1 = 0.008$ "

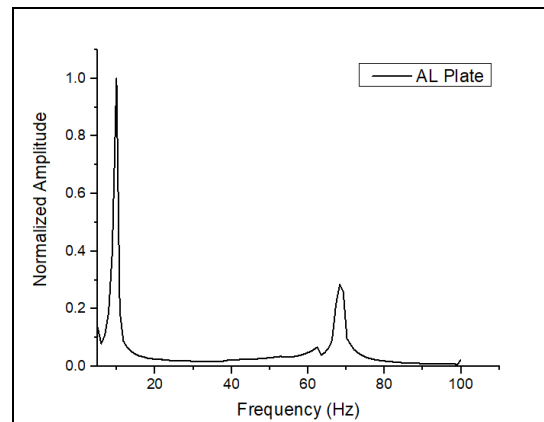


Fig. (5) The base plate experimental FRF for the first two bending modes

3.4. Measurement of the density of the plain plate material

A specimen of the plain plate material whose dimensions are 1.2x60x300mm is tested for the determination of its density; its weight is measured using a sensitive digital weight scale with sensitivity up to the third decimal number, where the weight is found to be 57 gram. Thus, the density of the plate material is

$$\rho = \frac{m}{V} = 2660 kg / m^3$$

Where " m " is the mass of the specimen and " V " its volume.

4. Mechanical Properties of the Damping Material

It is important to determine the mechanical properties of the damping material used (its Young's modulus and loss factor), which will facilitate the assessment of the performance of the (PTLD) treatment and its effect on the structural response.

4.1. Determination of Young's Modulus of the Damping Material

The elastic properties of the damping material layers can be determined from its stress-strain diagram. From this diagram, the slope of the stress-strain diagram within its linear elastic range represents Young's modulus. A tensile test is carried out on five samples of the damping material to draw its stress-strain diagram. The LRX-5K materials testing machine (LLOYD Instrument), is used to carry out the tensile tests for the prepared five samples of the damping material. This machine has a remote control software (DAMPAT software), which could acquire, record, analyze, store and print the test data. The

crosshead speed (strain rate) of the test machine is adjusted to 50-mm/min. Figure (6) shows schematic drawing of the instrument used in the tensile test.

The output of the tensile test, carried out by the above instrument, is the stress-strain diagram shown in Figure (7).

From Figure (7), Young's modulus of the damping material can be computed by applying Hooke's law at any point in the linear elastic range (shaded range) of that curve.

Considering Hooke's law

$$\sigma_d = E_d \varepsilon_d \tag{3}$$

After substitution the Young's modulus of the damping material used in the (PTLD) is $E_d = 0.986MPa$

Table (1) Mechanical and geometrical properties of the plain plate and the damping material used in the (PTLD) treatment

The damping layers that are formed from this material are pre-tensioned down the strain of $64000 \mu\varepsilon$ and perfectly bonded to the surfaces of the vibrating plate.

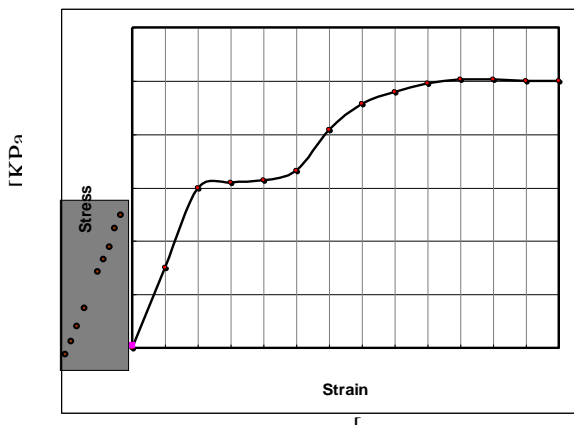


FIG. (7) STRESS-STRAIN DIAGRAM OF THE DAMPING MATERIAL

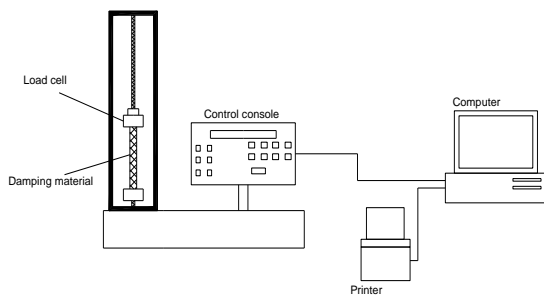


Fig. (6) LRX-5K material testing machine [LLOYD instrument]

4.2. Determination of the damping Loss Factor of the Damping Material

The mechanical properties of materials change with tension and compression. So, in order to determine an actual value for the damping loss factor of the damping material, it is necessary to perform the experiment with the damping material is not pre-tensioned. If the damping material is bonded into the surfaces of the plain plate without pre-tensioning, it will act as unconstrained layer damping treatment, (Plate/UCLD system), where the equation of the transfer function of the Plate/UCLD system is

$$|\alpha^u(\Omega, x)| = \sum_{n=1}^{\infty} \left[\frac{\left(2 \frac{\sigma_n^u \Omega^2}{\beta_n^u L} \right)}{\sqrt{\left[\left(\omega_n^u \right)^2 - \Omega^2 \right]^2 + \left[\left(\beta_n^u \right)^4 \left(\frac{2E_d' I_d \eta_d + E_3' I_3 \eta}{m^u} \right) + \frac{2G_d' \eta_d A_d \sigma_n^u \beta_n^u}{m^u L} \left(2 - \sigma_n^u \beta_n^u L \right) \right]^2}} \right] W_n^u(x) \tag{4}$$

Where

$$\left(\omega_n^u \right)^2 = \left(\beta_n^u \right)^4 \left(\frac{2E_d' I_d + E_3' I_3}{m^u} \right) + \frac{2G_d' A_d \sigma_n^u \beta_n^u}{m^u L} \left(2 - \sigma_n^u \beta_n^u L \right)$$

" $|\alpha^u(\Omega, x)|$ " is the magnitude of the transfer function of the Plate/UCLD system, which is the norm of the value of the relative displacement of the Plate/UCLD system element divided by the base displacement

$$|\alpha^u(\Omega, x)| = \left| \frac{w^u(x, t)}{y^b(t)} \right| \tag{5}$$

And the transfer function " $|\alpha^{ua}(\Omega, x)|$ " which represents the absolute displacement of the Plate/UCLD system element divided by the base displacement can be written as

$$|\alpha^{ua}(\Omega, x)| = \left| \frac{y^u(x, t)}{y^b(t)} \right| = \left| \frac{y^b(t) + w^u(x, t)}{y^b(t)} \right| = |1 + \alpha^u(\Omega, x)| \tag{6}$$

or

$$|\alpha^{ua}(\Omega, x)| = 1 + \sum_{n=1}^{\infty} \left[\frac{\left(2 \frac{\sigma_n^u \Omega^2}{\beta_n^u L} \right)}{\sqrt{\left[\left(\omega_n^u \right)^2 - \Omega^2 \right]^2 + \left[\left(\beta_n^u \right)^4 \left(\frac{2E_d' I_d \eta_d + E_3' I_3 \eta}{m^u} \right) + \frac{2G_d' \eta_d A_d \sigma_n^u \beta_n^u}{m^u L} \left(2 - \sigma_n^u \beta_n^u L \right) \right]^2}} \right] W_n^u(x) \tag{7}$$

Using the foregoing experimental set-up, an experiment to determine the damping loss factor of the cantilevered plate treated with unconstrained layer of the proposed damping material is performed. Two layers of the

damping material of dimensions 190x14x1mm are prepared, and perfectly bonded to the surfaces of the plain plate, then the whole structure is fixed into the steel base. The frequency is automatically swept over the frequency range of interest (3Hz up to 20 Hz), and the transfer function representing the absolute tip displacement of the treated plate to its base displacement is plotted. The measured and analyzed data is saved and plotted via the plotter. Figure (9) represents the transfer function of the cantilevered plate, treated with unconstrained layer of the proposed damping material. Also the data representing the tip displacement, which is measured by the inductive displacement pickup, is plotted, as shown in Figure (10). Figure (9) show that the 1st mode is symmetry about the vertical axis passing through the 1st natural frequency. This means that the half power method can be applied for the Plate/UCLD system model. Now, consider the nth mode of vibration of the Plate/UCLD system model, equation (7) can be written in the form

$$|\alpha_n^{ua}(\Omega, x)| = 1 + \frac{\left(2 \frac{\sigma_n^u \Omega^2}{\beta_n^u L}\right) W_n^u(x)}{\sqrt{\left[\left(\omega_n^u\right)^2 - \Omega^2\right]^2 + \left[\left(\beta_n^u\right)^4 \left(\frac{2E_d' I_d \eta_d + E_3' I_3 \eta}{m^u} + \frac{2G_d' \eta_d A_d \sigma_n^u \beta_n^u}{m^u L} (2 - \sigma_n^u \beta_n^u L)\right)\right]^2}} \quad (8)$$

and the transfer function representing the Plate/UCLD system tip displacement divided by the base displacement is given as

$$|\alpha_n^{ua}(\Omega, L)| = 1 + \frac{\left(2 \frac{\sigma_n^u \Omega^2}{\beta_n^u L}\right) W_n^u(L)}{\sqrt{\left[\left(\omega_n^u\right)^2 - \Omega^2\right]^2 + \left[\left(\beta_n^u\right)^4 \left(\frac{2E_d' I_d \eta_d + E_3' I_3 \eta}{m^u} + \frac{2G_d' \eta_d A_d \sigma_n^u \beta_n^u}{m^u L} (2 - \sigma_n^u \beta_n^u L)\right)\right]^2}} \quad (9)$$

it is possible to rewrite equation (9) in the form

$$|\alpha_n^{ua}(\Omega, L)| = 1 + \frac{Hr^2}{\sqrt{[1-r^2]^2 + \xi^2}} \quad (10)$$

where $H = 2 \frac{\sigma_n^u}{\beta_n^u} \frac{W_n^u(L)}{L}$, $r = \frac{\Omega}{\omega_n^u}$,

$$\left(\omega_n^u\right)^2 = \left(\beta_n^u\right)^4 \left(\frac{2E_d' I_d + E_3' I_3}{m^u}\right) + \frac{2G_d' A_d \sigma_n^u \beta_n^u}{m^u L} (2 - \sigma_n^u \beta_n^u L)$$

$$\xi = \left(\beta_n^u\right)^4 \left(\frac{2E_d' I_d \eta_d + E_3' I_3 \eta}{m^u \left(\omega_n^u\right)^4} + \frac{2G_d' \eta_d A_d \sigma_n^u \beta_n^u}{m^u \left(\omega_n^u\right)^4 L} (2 - \sigma_n^u \beta_n^u L)\right)$$

, and “ $|\alpha_n^{ua}(\Omega, L)|$ ” is the magnitude of the transfer function of the nth vibration mode of the Plate/UCLD system. From equation (10)

$$R_n^u(\Omega) = \frac{|\alpha_n^{ua}(\Omega, L)| - 1}{H} = \frac{r^2}{\sqrt{[1-r^2]^2 + \xi^2}} \quad (11)$$

and at resonance, the exciting frequency “ Ω ” equals the natural frequency of the system “ ω_n^u ”

$$\therefore r = 1 \quad (12)$$

Substitution of equation (12) into equation (11), it results

$$R_n^u(\omega_n^u) = \frac{1}{\xi} \quad (13)$$

and the magnitude of the power points is

$$R_n^u(\Omega_i) = \frac{R_n^u(\omega_n^u)}{\sqrt{2}} = \frac{1}{(\sqrt{2})\xi} \quad (14)$$

Let “ Ω_i ” is the frequencies of the power points, where “ $i = a, b$ ”

From equations (10) and (14)

$$R_n^u(\Omega_i) = \frac{R_n^u(\omega_n^u)}{\sqrt{2}} = \frac{1}{(\sqrt{2})\xi} = \frac{r_i^2}{\sqrt{[1-r_i^2]^2 + \xi^2}} \quad (15)$$

Where $r_i = \frac{\Omega_i}{\omega_n^u}$

from the equations (14) and (15)

$$\frac{1}{2\xi^2} = \frac{r_i^4}{[1-r_i^2]^2 + \xi^2} \quad (16)$$

$$\therefore (1 - 2\xi^2)r_i^4 - 2r_i^2 + (\xi^2 + 1) = 0 \quad (17)$$

Let $x_i = r_i^2$ (18)

Substitution of equation (18) into equation (17), it results in

$$(1 - 2\xi^2)x_i^2 - 2x_i + (\xi^2 + 1) = 0 \tag{19}$$

From the above quadratic equation, the roots are

$$x_i = \frac{2 \pm \sqrt{4 - 4(1 - 2\xi^2)(\xi^2 + 1)}}{2(1 - 2\xi^2)}$$

From the above equation

$$x_i = \frac{1 \pm \xi}{1 - 2\xi^2} \tag{20}$$

as “ ξ ” has a small value, therefore, the value of “ ξ^2 ” can be neglected

$$\therefore x_i = 1 \pm \xi \tag{21}$$

Therefore,

$$r_i^2 = 1 \pm \xi \tag{22}$$

At half power points, we have

$$r_a^2 = 1 - \xi \quad \text{and} \quad r_b^2 = 1 + \xi \tag{23}$$

From equation (23), we get

$$r_b^2 - r_a^2 = 2\xi \tag{24}$$

From equation (24)

$$\eta_n^u = 2\xi = \frac{\Omega_b^2 - \Omega_a^2}{\Omega_n^2} \tag{25}$$

Where “ η_n^u ” is the damping loss factor of the system.

$$\eta_n^u = 2\xi = 2(\beta_n^u)^4 \left(\frac{2E_d I_d \eta_d + E_3 I_3 \eta_1}{m^u (\omega_n^u)^4} \right) + \frac{4G_d \eta_d A_d \sigma_n^u \beta_n^u}{m^u (\omega_n^u)^4 L} (2 - \sigma_n^u \beta_n^u L) \tag{26}$$

From Figure (9) the value of the transfer function of the Plate/UCLD system and the value of the first resonant frequency is determined, where

$$\omega_1^u = 10.76 \text{ Hz}$$

Substitution by the given mechanical properties of the Plate/UCLD system in equation (25), the loss factor at the 1st resonance is “ $\eta_1^u = 0.17$ ”.

From equation (26), one can obtain the loss factor of the damping material used as

$$\eta_d = \frac{\eta_1^u m^u (\omega_1^u)^4 - 2(\beta_1^u)^4 E_3 I_3 \eta_1}{4G_d A_d \sigma_1^u \beta_1^u (2 - \sigma_1^u \beta_1^u L) + 4(\beta_1^u)^4 E_d I_d} \tag{27}$$

After substitution in equation (27), damping material loss factor is “ $\eta_d = 0.426$ ”.

5. Experimental Validation of the (PTLD) Technique

Using the foregoing experimental set-up, a group of experiments are performed on the cantilevered plate fully treated with pre-tensioned layer damping at different superficial forces, to show the effect of the superficial forces in damping out the vibration of the treated structures. Figure (8) shows the plate/PTLD assembly. The experimental results are compared with the theoretical results, which have been obtained in to validate the theoretical analysis, and to prove the high damping characteristics of the new technique. Now, refer to Figure (9), which shows the comparison between the magnitude of the transfer function of the plate with the unconstrained layer damping of the proposed damping material and the transfer function of the cantilevered plain plate. This comparison shows the attenuation percentage produced by the damping material without pre-tensioning and the attenuation percentage is calculated as follows

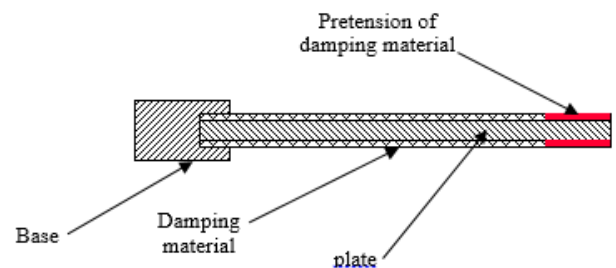


FIG. (8) PLAIN PLATE WITH PRETENSION LAYER ASSEMBLY

$$\Delta_n^t(\omega_n) = \frac{|\alpha(\omega_n)| - |\alpha^t(\omega_n)|}{|\alpha(\omega_n)|} 100\%$$

The attenuation percentage, due to the unconstrained layer UCLD is

$$\Delta_1^t(\omega_1) = 60.8\%$$

Figures (10, 11, 12, and 13) shows the transfer function at the tip of the Plate/PTLD system at different superficial force values and the attenuation percentage is calculated. From Figure (11) the attenuation percentage, due to the PTLD layer at superficial forces equal, 10 N, 20 N, 40 and

60 N are calculated and the obtained percentage is given by $\Delta_1^t(\omega) = 59\%$, $\Delta_1^t(\omega) = 72\%$, $\Delta_1^t(\omega) = 76\%$ and $\Delta_1^t(\omega) = 84\%$ respectively.

The effect of temperature and frequency on the Young's modulus, shear modulus and loss factor of the damping material should be considered, because the rubber-like materials behave as viscoelastic materials. But for the present study all the experiments have been carried out at constant temperature of 25° c, and the frequency sweep ranges of excitation are small enough to keep the values of the mechanical properties of the damping material with no change during the experiments. Table (2) shows a comparison between the theoretical and the experimental attenuation percentages at the same superficial force values. Since the level of the exciting force is kept constant during sweep test of either plain plate or Plate/PTLD system, it is possible to show the effectiveness of the new technique by comparing the FRF of amplitude of the plain plate and the Plate/PTLD system. Figure (13) shows a comparison between the (FRF) values of the Plate/PTLD system tip displacements at different superficial forces, which indicates the high damping capabilities of the new technique. The high damping characteristics of the pre-tensioned layer damping technique and the capability of the new technique in the reduction of the tip displacement at resonant frequencies can easily be seen from this figure. It is also seen that the shift in the structural resonant frequency is very small, which indicates that the proposed technique does not change the mechanical properties of the system.

SUPERFICIAL FORCE " F_0 " [N]	10	20	40	60
Theoretical attenuation Percentage " $\Delta_1^t(\omega_1)$ " [%]	61	70	75	82
Experimental attenuation Percentage " $\Delta_1^t(\omega_1)$ " [%]	59	72	76	84

Table (2) Comparison between theoretical and experimental attenuation

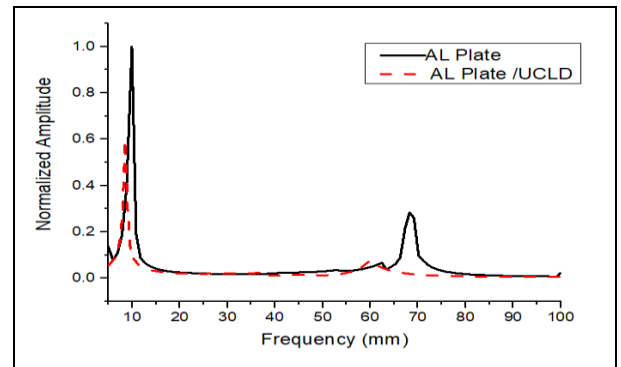
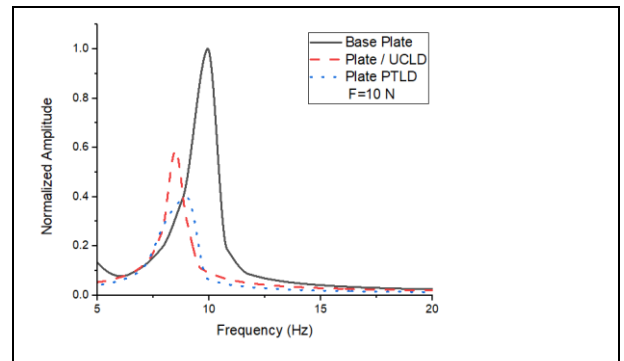
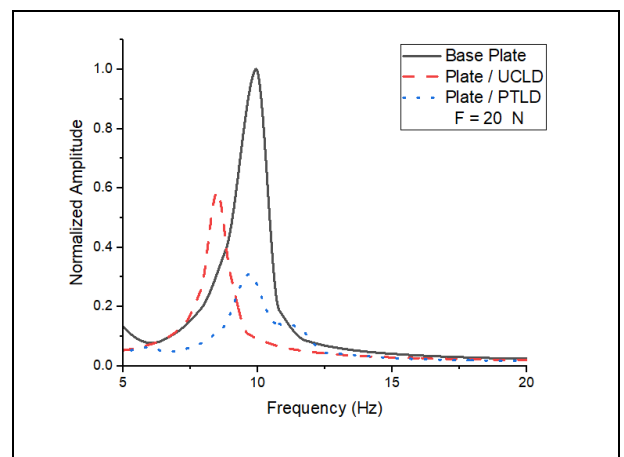


Fig. (9) The plate experimental FRF for the first two bending modes



Fig(10) The comparison between the AL plate and the plate /PTLD system with force F=10 N for the first bending mode



Fig(11) The comparison between the AL plate and the plate /PTLD system with force F=20 N for the first bending mode

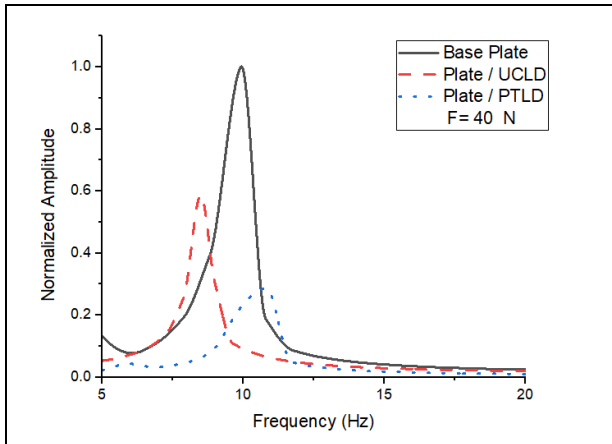


Fig. (12) The comparison between the AL plate and the plate /PTLD system with force $F=40$ N for the first bending mode

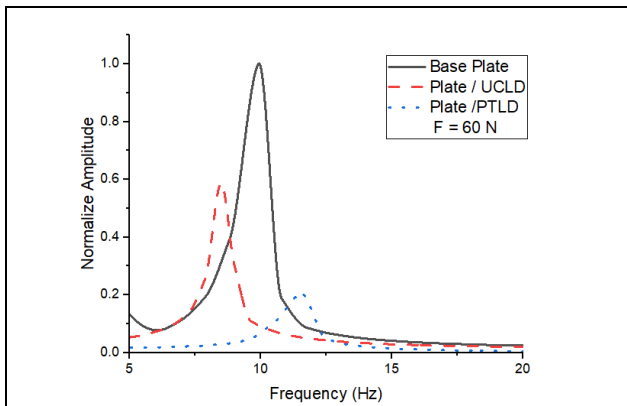
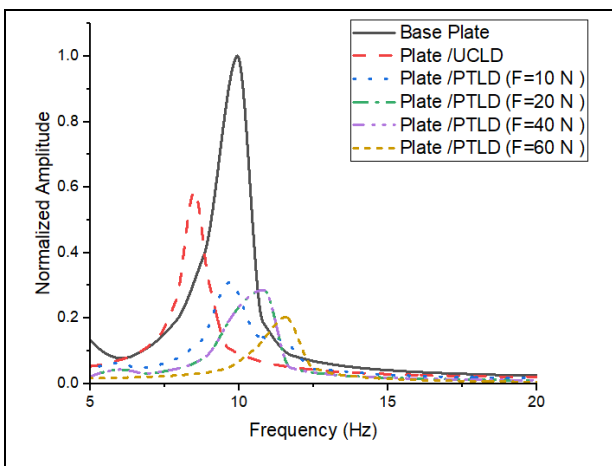


Fig. (13) The comparison between the AL plate and the plate /PTLD system with force $F=60$ N for the first bending mode



Fig(13)The comparison between the AL plate and the plate /PTLD system with different forces for the first bending mode

6. CONCLUSIONS

In the present paper, a new passive control technique for suppression of the lateral vibrations of a flexible base excited cantilevered plate, is proposed.

This new technique is a sort of artificial damping techniques, which is based on the theory of energy dissipation from vibrating systems.

The proposed new technique, which is called Pre-tensioned layer damping (PTLD), consists of a conventional passive unconstrained damping layer, which is subjected to a slight pre-tensioning that is translated into a uniformly distributed forces on the superficial fibers of the vibrating structures. These forces have a complex form, due to its direct dependency on the Young's modulus of the damping material, which by its turn, has a Rheological behavior due to viscoelasticity. The vertical components of the real part of these complex forces always tends to straighten the elastic line of the vibrating plate by increasing its stiffness, while the imaginary part has a damping nature depending on the initial strain induced in the damping layer as well as the damping loss factor of the damping material. These two parts of the superficial forces play an important role in the reduction of the plate vibration amplitudes. The mechanical properties of the structure and the used damping material are determined, which enabled the theoretical analysis for a specific base structure and damping materials. From experimental results, the attenuation percentages corresponding to different levels of superficial forces were calculated. A good agreement between the theoretical predictions and the experimental results was ascertained.

The following conclusions may be drawn through the experimental and the theoretical study presented in this thesis

A new simple, reliable and low cost technique for the suppression of vibration of flexible structures is developed.

- 1- The new proposed model has shown a major advance in the attenuation of the vibration amplitude using very simple technique, which enhances the system reliability avoiding the complications of control devices used in the case of the ACLD technique and the limitation of damping in the case of PCLD technique.
- 2- The higher the elastic superficial forces in the pre-tensioned layer damping material, the higher are the attenuation percentages and the damping effectiveness.

ACKNOWLEDGMENT

I wish to express my sincere and deep gratitude to my supervisor Prof.Dr. Adel Abdelrazek Omar for his generous support during the whole process of this research.

REFERENCES

1. Elias, S. and V. Matsagar, Research developments in vibration control of structures using passive tuned mass dampers. *Annual Reviews in Control*, 2017. **44**: p. 129-156.
2. Ude, C.O., Experimental Study of Segmented Constrained Layer Damping in Rectangular and Sinusoidal Beams. 2020, University of Maryland, College Park.
3. Li, W., et al., A reduced passive constrained layer damping finite element model based on the modified improved reduced system method. *Journal of Sandwich Structures & Materials*, 2019. **21**(2): p. 758-783.
4. Sahoo, S. and M. Ray, Analysis of smart damping of laminated composite beams using mesh free method. *International Journal of Mechanics and Materials in Design*, 2018. **14**(3): p. 359-374.
5. Thompson, D.J., G. Kouroussis, and E. Ntotsios, Modelling, simulation and evaluation of ground vibration caused by rail vehicles. *Vehicle System Dynamics*, 2019. **57**(7): p. 936-983.
6. Ghaedi, K., et al., Invited Review: Recent developments in vibration control of building and bridge structures. *Journal of Vibroengineering*, 2017. **19**(5): p. 3564-3580.
7. Wang, Y. and X. Li, 4D printing reversible actuator with strain self-sensing function via structural design. *Composites Part B: Engineering*, 2021. **211**: p. 108644.
8. Gentili, D., et al., Polymorphism as an additional functionality of materials for technological applications at surfaces and interfaces. *Chemical Society Reviews*, 2019. **48**(9): p. 2502-2517.
9. Jayathilaka, W.A.D.M., et al., Significance of nanomaterials in wearables: a review on wearable actuators and sensors. *Advanced Materials*, 2019. **31**(7): p. 1805921.
10. Agrawa, Y., et al., Sustainable structures for smart cities and its performance evaluation. *Int Res J Eng Technol*, 2017. **4**.
11. Mohamed, A., A. Hassan, and A. Omer. Passive vibration damping of a cantilever plate. in IOP

Conference Series: Materials Science and Engineering. 2020. IOP Publishing.